THE EUROPEAN PHYSICAL JOURNAL D

Ionization of Rydberg atoms in THz-laser fields at the transition from low to high scaled frequencies

S. Ring[a], B. Schmidt[b], and H. Baumgärtel

Freie Universität Berlin, Institut für Physikalische und Theoretische Chemie, Takustr. 3, 14195 Berlin, Germany

Received: 17 February 1998 / Revised: 20 April 1998 / Accepted: 21 April 1998

Abstract. We have studied the ionization of Rydberg–excited xenon atoms in THz-laser fields and by quantum dynamical calculations. The experimental threshold laser field strength for 10% ionization probability follows an $n^{*-1.68}$ ($\omega/2\pi$ =1.04 THz) dependence (n^* effective principal quantum number) with additional weak resonance structures and shows that ionization does not occur by a Landau–Zener mechanism. At scaled frequencies of $\Omega = 0.71$ to 5.6 the simulated threshold fields for ionization in oscillatory fields show a dependence on the principal quantum number n of $n^{-4.1}$ to $n^{-1.35}$.

PACS. 32.80.Rm Multiphoton ionization and excitation to highly excited states (*e.g.*, Rydberg states) – 42.50.H Strong-field excitation of optical transitions in quantum system; multiphoton processes; dynamic Stark shift

1 Introduction

The interaction of Rydberg atoms with electric fields, both static and time dependent, has been intensely studied because these systems allow the detailed investigation of electron dynamics at the transition from quantal to classical behavior. The ionization in static electric fields can be interpreted in terms of the classical lowering of the ionization potential in the external field and quantum mechanical tunneling, leading to the escape of electrons from a critical quantum number on. The ionization of Rydberg atoms in time dependent periodic fields has mostly been studied in the microwave region [1–3]. In microwave fields ionization occurs already at field strengths much lower than those required in static fields. At the same time, in many cases hundreds of microwave photons are necessary to ionize a Rydberg state with the ionization being interpreted as a sequence of Landau–Zener transitions between adjacent states of the Stark manifolds [2,3]. The ionization behavior in static and in microwave fields is characterized by ion yield curves with threshold fields depending on n, scaling as n^{-4} and n^{-5} for the static and the microwave case, respectively. Most of the microwave experiments were performed in the regime of low scaled frequency $\Omega = n^3\omega \ll 1$, where the electric field is slowly varying compared with the Kepler period $T_K = 2\pi n^3$ of the Rydberg electron. Only in very few experiments the range of $\Omega \approx 1$ and beyond has been explored. This has been realized either by investigating higher Rydberg states in 36-GHz microwave fields ($\Omega \leq 2.8$) [1] or by using far–infrared (FIR) laser fields. The latter approach has been pursued by Noordam *et al.* using frequencies above 3.3 THz (110 cm^{-1}) to investigate *resonant* multiphoton ionization of Rydberg states and the Cooper minima occuring therein [4]. The regime of $\Omega \approx 1$ has also been investigated in nonperiodic electric fields where half–cycle electromagnetic pulses (HCPs) have been applied to ionize Rydberg atoms. For a HCP with pulse width T_d of the order of the Kepler period, the threshold fields for ionization show an n^{-2} dependence [5], approaching an n^{-1} dependence in the ultrashort pulse limit [6,7].

In the present work the multiphoton ionization of Rydberg states is explored using a far–infrared gas laser operating at 1.04 THz (34.7 cm^{-1}) and by quantum dynamical calculations.

2 Experimental

The experimental setup consists of a time–of–flight mass spectrometer combined with two dye lasers, operating in the visible and in the near UV, and a far–infrared gas laser. The FIR light source is an optically pumped gas laser [8], which consists of a gas cell filled with CH_3F. Using the CO_2 9R20 pump line, one obtains radiation at 1.04 THz with a pulse width of 50 ns. The FIR laser beam was focused by a parabolic mirror (f = 250 mm) into the excitation region of the ion optics. Its spot size is much bigger than the region where the Rydberg atoms are formed, and we assume that all Rydberg atoms experience the same FIR field intensity. Xenon atoms are excited to Rydberg

[a] *Present address:* Department of Environmental Sciences, Weizmann Institute of Science, Rehovot 76100, Israel
[b] e-mail: bschmidt@chemie.fu-berlin.de

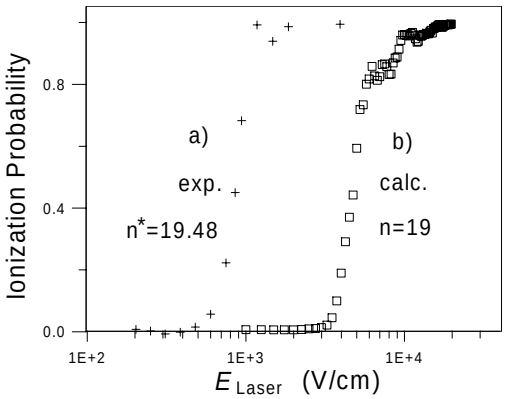

Fig. 1. Experimental (a) and simulated (b) ionization onset curves as a function of FIR laser field strength.

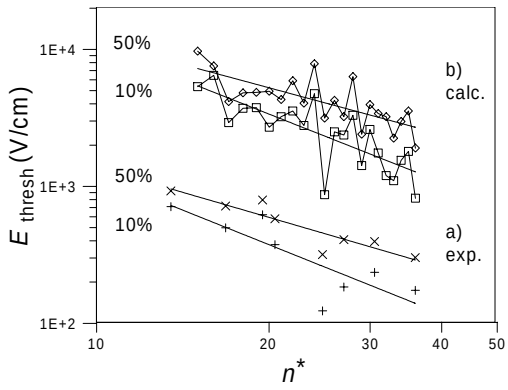

Fig. 2. Experimental (a) and simulated (b) threshold laser fields for 10% and 50% ionization probability as a function of the effective principal quantum number n^*. The threshold fields scale as $n^{-1.13}$ (calc., 50%), $n^{-1.65}$ (calc., 10%), $n^{*-1.22}$ (exp., 50%) and $n^{*-1.68}$ (exp., 10%); ($n = n^*$ in the simulations).

states using a 2+1 excitation scheme. Two–photon excitation to the $^2P_{3/2}5p^5 6p$ state is followed by absorption of a third photon to excite the atoms to $^2P_{3/2}nd$ Rydberg states. After 100 ns the Rydberg states are exposed to the FIR laser field. After another time delay of 1 μs a static field of 50 V/cm is applied to extract the ions into the drift tube of the time–of–flight apparatus, where they are detected on a microchannel plate detector. The assignment of the individual Rydberg states was based on a VUV absorption spectrum [9]. For our experiments, we chose the $n^*d(3/2)$-Rydberg series ($n^* = 15$ to 35) converging to the first ionization potential at 97833.75 cm^{-1}. Only comparatively low lying Rydberg states were measured, since very high Rydberg states could cause systematic errors due to the extraction field leading to ionization for all states above n^*=50. By varying the intensity of the ionizing FIR laser, we obtained ion yield curves for different n^*. All measured ion yield curves show a slowly rising onset with a saturation region at higher pulse intensities.

As an example, the ion yield curve for n^*=19.48 is shown in Figure 1a. The central part of the onset can be fitted with a power law $I \propto P^m$ (I ion signal, P pulse intensity), with an exponent of m=2.8. From the ion yield curves for different n^* we extracted field values for 10% and 50% ionization probability. In Figure 2a the threshold electric fields E_{thresh} as a function of n^* are shown. The resulting curves can be fitted with n^*–dependencies of $E_{thresh} \propto n^{*-1.68}$ and $E_{thresh} \propto n^{*-1.22}$ for 10% and 50% ionization, respectively. The curve in the logarithmic plot of E_{thresh} *vs.* n can not be expected to be linear in the investigated n-range. Hence, we interpret the obtained dependence of the threshold field as a linear approximation by a tangent near the center of the E_{thresh} *vs.* n curve at $n = 25$, corresponding to a scaled frequency $\Omega = 2.37$. The different n^*–dependencies for the 10% and 50% threshold fields correspond to the observed broadening of the ionization onset region with increasing n^*. The 10% threshold fields for all n^* are smaller than those required for ionization in static fields.

3 Quantum Simulations

To support the interpretation of the experimental data quantum dynamical simulations have been carried out. The time dependent Schrödinger equation for the radial wavefunction in position space representation can be written (in atomic units) as

$$i\frac{\partial}{\partial t}\psi(r,t) = \left[\hat{T} + \hat{V}_{eff}(r,t)\right]\psi(r,t). \tag{1}$$

Here the radial part of the kinetic energy is given by

$$\hat{T} = -\frac{1}{2}\frac{\partial^2}{\partial r^2} \tag{2}$$

and the effective potential is

$$\hat{V}_{eff}(r,t) = -\frac{1}{r} + \frac{\ell(\ell+1)}{2r^2} - r\mathcal{E}(t) \tag{3}$$

where the second and third term on the r. h. s. describe the centrifugal barrier and the interaction between the atomic dipole moment and an external (time–dependent) electric field in the semiclassical dipole approximation, respectively [10]. The laser pulses are assumed to be of the form

$$\mathcal{E}(t) = \mathcal{E}_0 \sin^2\left(\frac{\pi t}{2T}\right)\cos(\omega t), \quad 0 \le t \le 2T \tag{4}$$

in which $\mathcal{E}_0$ and ω are the amplitude and the frequency of the pulse, respectively. In our nonperturbative approach we solve this equation numerically using methods originally developed for the field of quantum molecular dynamics [11] which were also applied to simulate the time evolution of a Rydberg wavepacket in microwave fields [12]. The radial wavefunction $\psi(r,t)$ is represented on an equally spaced grid (consisting of 2048 points covering the range up to $r = 500$ nm) which facilitates evaluation

of the kinetic energy operator by fast Fourier transform (FFT) techniques. In addition, we use a negative imaginary potential to absorb the outgoing part of the wave function at the end of the grid. To avoid numerical instabilities caused by the steep well of the effective potential for small angular momenta, we chose here a relatively large value of $\ell = 14$. However, in principle this problem could also be circumvented using the recently published mapped Fourier method [13]. For simplicity, we assume $\Delta\ell = 0$ and we neglect polarization or orientation effects in the present work. For sufficiently small time steps $\Delta t = 10$ fs, the potential energy operator of equation (3) can be regarded time–independent thus permitting an easy evaluation of the time evolution operator by the split–operator scheme [14]

$$\psi(t+\Delta t) = e^{-i\Delta t\hat{H}}\psi(t)$$
$$= e^{-i\frac{\Delta t}{2}\hat{T}}e^{-i\Delta t\hat{V}_{eff}}e^{-i\frac{\Delta t}{2}\hat{T}}\psi(t) + \mathcal{O}(\Delta t)^3. \quad (5)$$

In our simulations we assumed laser pulses of T=90 ps duration. After the end of the laser pulse, the propagations were continued for another 10 ps to finally determine the ionization probability. The actual laser pulse of the experiment could not be simulated due to its long duration of ≈ 50 ns. In order to be compatible with the experimental situation where all states for $n > 50$ are ionized by static fields, we determined the survival probability (for atoms not being ionized) by projecting the time dependent wavefunction on the first 50 eigenstates of the effective potential and defining the remainder as ionization probability.

We performed simulations for FIR pulses of various intensities and frequencies. The calculated ion yield curve for $n = 19$ and 1.04 THz is given in Figure 1b. The central part of the curve can be fitted by an $I \propto P^m$ law with an exponent of $m = 3.5$, which is in reasonable agreement with the experimental value of 2.8. Ion yield curves have been simulated for $n = 15$ to 35 and the threshold laser fields for 10% and 50% ionization probability have been extracted. The results for $\omega/2\pi = 1.04$ THz are plotted in Figure 2b. The curves can be fitted by an $E_{thresh} \propto n^s$ scaling law with exponents $s = -1.65$ (-1.13) for 10% (50%) ionization. Contrary to the experimental data, where the sparsity of data points (together with possible resonances) make it difficult to determine a small change of the scaling exponent s for different n^* values, the calculated data points clearly show such a change. The scaling law exponent decreases with increasing n (10% ionization: $15 < n < 25$: $s = 1.88$, $26 < n < 35$: $s = 1.28$). Again, the scaling law exponent for $15 < n < 35$ is therefore taken as a slope of a tangent near the center of the curve at $n = 25$.

Note that the E_{thresh} *vs.* n curves obtained from the simulations exhibit small oscillations which will be discussed later. The experimental laser field strength differs in all cases from the calculated values by a factor of ≈ 8. This appears to be a consequence mainly of difficulties in the determination of the experimental field strengths, but also of the short simulation times (compared to the long–pulse excitation in the experiment). Nonetheless, the good agreement of the experimental with calculated slopes for the ion yield and for the threshold field curves shows that our numerical model indeed describes the essential physical behavior of the system correctly. In addition to the E_{thresh} *vs.* n curve for 1.04 THz, we carried out simulations for FIR pulses of 2.4 THz, 0.6 THz, and 0.3 THz, corresponding to $\Omega = 5.6$, 1.42, and 0.71 for $n = 25$. The resulting scaling exponents for 10% ionization were $s = -1.35$, -2.11, and -4.1.

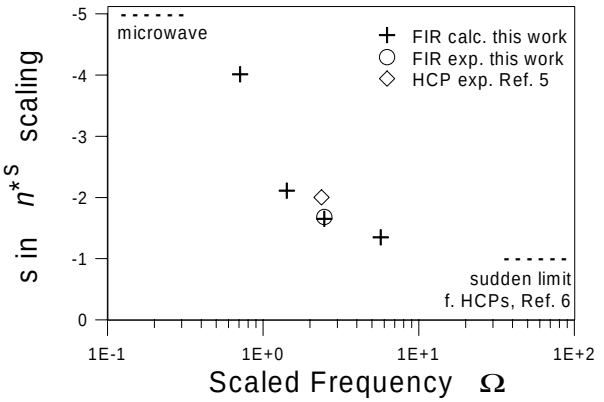

Fig. 3. Experimental and calculated scaling exponents of the threshold fields (10% ionization probability) as a function of the scaled frequency Ω. For comparison, scaling exponents for ionization in microwaves and in HCPs have been added at their approximate Ω values.

4 Discussion

In the present work we have extended the range of scaled frequency Ω of earlier experiments, which were carried out using microwave fields, to $\Omega \leq 5.6$ using THz laser fields. The weak laser fields $E < E_0$ (E_0 attractive field of the nucleus) and scaled frequencies of $\Omega \leq 5.6$ are close to the multiphoton ionization regime. In this regime, where perturbation theory is commonly used to describe multiphoton processes, the number of photons required for ionization, giving the actual multiplicity of the process, can be extracted from the slope of the ion yield curve as a function of the intensity in a log–log plot, assuming that no intermediate resonances occur. The experimental slope of 2.8 (calc. 3.5) in a 1.04-THz field deviates considerably from the value which one might expect for a simple multiphoton ionization scheme for a Rydberg state where 9 photons are required for ionization (n^*=19.48). This clearly shows that nonperturbative calculations are necessary to describe the ionization. Furthermore, the ionization of Rydberg states in nonresonant FIR laser fields is found to be distinctly different from the ionization in microwave fields. The scaling law exponents s between -1.35 and -4.1 obtained both in experiment and simulations show that a Landau–Zener mechanism, leading to $s = -5$, as it is commonly used to describe the ionization of Rydberg states in microwave fields ($\Omega \ll 1$), can be excluded for the THz-frequencies considered here.

The different findings for nonresonant oscillatory fields are summarized in Figure 3, where various experimental and calculated scaling law exponents are plotted as a function of the scaled frequency Ω. The scaling exponent s decreases from the value for microwave fields with increasing Ω and seems to approach $s = -1$ at high scaled frequencies. The scaling exponents obtained in this work can be compared with those for ionization by a 500 fs-HCP with a central frequency of ≈ 1 THz [5,16] (corresponding to $\Omega \simeq 2.37$ at n=25), and for HCP ionization in the ultrashort pulse limit [6,7], both given in Figure 3. The scaling exponent of -2 for the 500 fs-HCP fits well with the experimental and calculated scalings of the present work [15]. FIR ionization seems to approach the same scaling exponent as HCP ionization in the limit of ultrafast excitation ($\Omega \gg 1$). A further similarity for HCPs and FIR ionization is the broadening of the ionization onset curves with increasing quantum number n. For the 500 fs-HCP in reference [5], the scaling exponent for 50% ionization probability (-1.5) is lower than that for 10% ionization (-2), similar to our results in FIR-fields (10%:-1.68, 50%:-1.22). These results indicate that there is no principal difference between the ionization mechanism in periodic fields and in the HCP experiments of reference [5] concerning the time scale of excitation, expressed by the scaled frequency Ω.

Classical dynamics describes very well the microwave ionization of Rydberg states at low scaled frequencies and has also been employed by means of a momentum transfer model to interpret the HCP experiments in reference [5]. However, quantum effects can be expected to play a role in oscillatory fields. For the frequencies used here, a weak resonance structure appears superimposed on the simulated E_{thresh} *vs.* n–curves (see Fig. 2). These minima (maxima) are caused by accidental quasi–resonances of the photon energy with a transition from the initial to a higher (lower) Rydberg state ($\Delta n = \pm 2, 3$ in this case), indicating that in favorable cases resonant absorption (stimulated emission) is the first step towards ionization. The resulting Rydberg state is then ionized at lower (higher) electric field strength. Our experimental data on xenon show only one feature at $n^* \approx 24$ which can clearly be assigned to a quasi–resonance. Small oscillations due to quasi–resonances could also be expected to appear in an s *vs.* Ω curve such as that in Figure 3. The scaling exponents therein, however, are determined from the slopes of E_{thresh} *vs.* n curves where the laser field is nonresonant for most of the n values so that small resonances are levelled out. The resonances occuring in our simulations, however, become less pronounced upon decreasing the scaled frequency thus illustrating the transition from higher Ω values, where resonances and quantal behavior are dominant, to the low Ω regime where classical models suffice to describe the dynamical behavior. In conclusion, we have determined the threshold field dependence of Rydberg ionization for $0.71 < \Omega < 5.6$, for the first time using a far–infrared gas laser. The ionization behavior in nonresonant laser fields resembles that observed in HCP experiments but in addition shows quantum effects.

Financial support by the Deutsche Forschungsgemeinschaft (SFB 337) is gratefully acknowledged. We thank B. Wassermann for assistance in performing the experiments.

References

1. E.J. Galvez, B.E. Sauer, L. Moorman, P.M. Koch, D. Richards, Phys. Rev. Lett. **61**, 2011 (1988).
2. C.R. Mahon, J.L. Dexter, P. Pillet, T.F. Gallagher, Phys. Rev. A **44**, 1859 (1991).
3. T.F. Gallagher, *Rydberg Atoms* (Cambridge University Press, Cambridge, 1994).
4. J.H. Hoogenraad, R.B. Vrijen, P.W. van Amersfoort, A.F.G. van der Meer, L.D. Noordam, Phys. Rev. Lett. **75**, 4579 (1995).
5. R.R. Jones, D. You, P.H. Bucksbaum, Phys. Rev. Lett. **70**, 1236 (1993).
6. M.T. Frey, F.B. Dunning, C.O. Reinhold, J. Burgdörfer, Phys. Rev. A **53**, 53 (1996).
7. C.O. Reinhold, M. Melles, H. Shao, J. Burgdörfer, J. Phys. B **26**, L659 (1993).
8. C. T. Gross, J. Kiess, A. Mayer, F. Keilmann, IEEE J. Quantum Electron. **23**, 377 (1987).
9. K. Yoshino, D.E. Freeman, J. Opt. Soc. Am. B **2**, 1268 (1985).
10. R. Loudon, *The Quantum Theory of Light* (Clarendon, Oxford, 1973).
11. R. Kosloff, Ann. Rev. Phys. Chem. **45**, 145 (1994).
12. T. Jiang, S. Chu, Comp. Phys. Comm. **63**, 482 (1991).
13. E. Fattal, R. Baer, R. Kosloff, Phys. Rev. E **53**, 1217 (1996).
14. M.D. Feit, J.A. Fleck, A. Steiger, J. Comput. Phys. **47**, 412 (1982).
15. In test simulations with our numerical procedure for a 500 fs-HCP we obtained a scaling exponent of -2.1 ($n = 25$), close to the results in reference [16].
16. A. Bugacov, B. Piraux, M. Pont, R. Shakeshaft, Phys. Rev. A **51**, 1490 (1995).